1-1-1970

Massive and martensitic transformations in very dilute iron-carbon alloys.

Robert James Ackert
University of Windsor

MASSIVE AND MARTENSITIC TRANSFORMATIONS IN VERY DILUTE IRON-CARBON ALLOYS

A Thesis

Submitted to the Faculty of Graduate Studies
through the Department of Engineering Materials
in Partial Fulfilment of the Requirements
for the Degree of Master of Applied
Science at the University of Windsor

by

Robert James Ackert

Windsor, Ontario
1970

FP 16932

Chairman

Committee

320114

ABSTRACT

The results of transforming very dilute iron-carbon alloys (6-180 ppm by weight of carbon) at cooling rates up to 115,000 ^{o}C/sec. are presented with observations of massive and martensitic transformations in the same alloys at different cooling rates. It is observed that the martensite start temperature increases very rapidly with small decreases in carbon content in the alloy range investigated and that the massive start temperature increases less rapidly. An M_s temperature of 750^{o}C is established for the Fe-15 ppm C alloy (the most dilute alloy for which reproduceable results were obtained) and it is suggested that the M_s and massive tranformation temperatures coincide at 770^{o}C (the Curie temperature) for "pure" iron.

ACKNOWLEDGEMENTS

The present author wishes to extend his appreciation to Dr. J.G. Parr for his capable direction and for the opportunity to study under him.

Acknowledgements are also extended to Prof. R.G. Billinghurst for his able departmental guidance and to Mr. R. Hamilton for his assistance in preparing the iron-carbon alloys used and to whom the present author is indebted for the information contained in Appendix I. In addition, special recognitions are extended to Dr. G.W.P. Rengstarff of Battelle Memorial Institute and to Dr. D.J. Blickwede of the Bethlehem Steel Company for their supplying the necessary high purity iron at no cost and for arranging for the carbon analyses; and to Mr. F. Huber of Battelle Memorial Institute for his excellent co-operation in carrying out the carbon analyses.

Acknowledgements are also extended to the National Research Council for the bursary granted to the author and to the Defence Research Board who sponsored the work under D.R.B. grant no. 9535-16.

TABLE OF CONTENTS

LIST OF FIGURES

LIST OF TABLES

INTRODUCTION

I--General

The metal iron has had an influence of unique importance on the history of our society. Its earliest general usage is ranked of such note that an age is named after it and, in recent times, iron and its alloys have had greater commercial significance than any other group of alloys.

Iron, like titanium, zirconium, thallium and sodium, transforms from a body-centred-cubic structure at high temperatures to a close packed structure at lower temperatures. Zener (1) explains the high temperature stability of the less densely packed structure by considering the unusually large amplitude of vibration associated with its (110) ($\bar{1}$10) shear-strain co-ordinate and hence its very high entropy factor (s). The criterion for the stability of a phase is that its free energy (G) be lower than that of any possible alternate phase. If U is the internal energy,

$$G = U-TS+PV$$

where

T is temperature,

P is pressure

V is volume

Thus a large value for the entropy term S implies a

rapid decrease in free energy with increasing temperature. The body-centred-cubic structure will therefore be more stable at high temperatures (ΔS being of greater effect than ΔV) than the close-packed structure which has a lower entropy term. However, iron is stable in the body-centred-cubic structure at both high and low temperatures and is stable in the close-packed face-centred-cubic structure only in the intermediate temperature range 910° - 1389°C.

Kaufman, Clougherty and Weiss (2) have postulated that the formation of the f.c.c. iron structure involves two magnetic spin states separated by a small energy gap. The thermally activated population of the upper energy state, which occurs as the temperature increases, imparts an extra entropy to the f.c.c. iron which in turn results in its stability above 910°C. In the free energy expression, the entropy term resulting from magnetic disordering at the Curie point is multiplied by an increasing value of T and eventually overrides the entropy of the two-spin state of the f.c.c. structure at 1389°C. According to this viewpoint, the lower b.c.c. → f.c.c. transformation could be expected to occur at the Curie point. The fact that it actually occurs 150°C above it has been attributed by Zener (3) to a correlation phenomenon between neighbouring spins, a contention that receives some support due to iron's position near

the end of the transition group of elements in the periodic table.

The magnetic-spin-state approach to the b.c.c.→ f.c.c.→ b.c.c. transformations in iron would suggest that the low temperature b.c.c. (α) iron and the high temperature b.c.c. (δ) iron are the same structure. This consideration receives some support from thermodynamics and thermal expansion data, electrical resistivity measurements and the effects of some alloy additions to iron (iron can be alloyed so that the b.c.c. structure extends from room temperature to the solidus). However, since free energy changes associated with transformation phenomena are usually very small, first principle calculations based on quantum theory must be very exact before a change in relative crystal stabilities can be predicted. It is not surprising, therefore, that there is not yet a fully accepted theory of the b.c.c.→f.c.c.→ b.c.c. transformations in iron (4).

The δ(b.c.c.)→γ(f.c.c.)→α(b.c.c.) transformations discussed take place when the cooling rates involved are sufficiently low that equilibrium conditions are approached. However, non-equilibrium cooling from the γ (f.c.c.) phase is of very great interest not only because of the scientific curiosity aroused by the martensitic and massive transformations that may result, but also because the strengthening mechanisms in iron alloys are dependent on rapid cooling.

Although considerable energies have been expended in the pursuit, satisfactory conclusions concerning the behavior of the massive and martensitic reactions in pure iron have not been agreed upon because it has been particularly difficult to obtain "pure" iron free from the influence of carbon, an element that greatly influences these reactions. It is the purpose of the present investigation to explore the effects of small carbon additions on the massive and martensitic transformations in very dilute iron-carbon alloys.

II--The Martensitic Transformation

The term "martensite" was originally used only in reference to the microstructure obtained in quenched steels. Although ferrous martensites are still commercially the most important, the original definition is now much too restrictive: many other alloy systems have been shown to display similar transformations. Table I by Barrett (28) gives a partial list of these other systems.

Recent investigators generally use definitions for martensite that emphasize conformity to the following conditions (6,7,8):

(a) The transformation is accompanied by a shape change corresponding to a homogeneous tilt on a free metal surface, which is caused by a shear displacement of atoms.

(b) All atomic displacements are limited to less than one interatomic distance. This can be taken to mean that the transformation is diffusionless.

Bilby and Christian (8) emphasize that the diffusionless nature of the reaction is a consequence of the shear strain that produces the homogeneous tilt and therefore they put forward the "surface rumpling" criterion for the recognition of a martensite transformation.

In addition to the features emphasized in the definitions, the following features are generally

associated with martensite:

1) The transformation takes place without a change in the chemical composition of the parent phase due to the diffusionless nature of the reaction (6,9).

2) Atomic interchange does not play a significant role in the transformation as evidenced by the fact that ordered phases remain ordered after a martensite reaction (10).

3) It follows from #2 that the atoms must move in some orderly and co-ordinated fashion, which introduces the concept of an invariant plane in a deformation that carries the points of one lattice into those of the other (10,11). If this invariant plane remains unrotated after the transformation, it is also the habit plane of the martensite plates (the habit phase being a plane that remains unrotated and undistorted during the transformation). This shear component of the transformation is parallel to the habit plane, and the dilatational component is perpendicular to it, resulting in a matrix-martensite interface that remains unrotated (8).

4) In some martensites, a degree of atomic shuffling in addition to homogeneous shear is necessary to account for atomic positions relating to the deformed lattice (11,12).

5) The velocity of formation of a martensite is of

the same order as the velocity of sound in the material even at extreme cryogenic temperatures ($\lesssim 4^{o}K$). This suggests a very small activation energy for the process and a maintained coherency between the product and parent phases during growth (6,11,13,14).

6) Martensite may form in a sudden burst over entire regions of the microstructure over very small temperature ranges or may grow evenly. The "burst phenomenon" is similar to a chain reaction where the stress produced by one plate assists in the nucleation of the next plate, with the result that plates are often observed to propagate end to end (6,11,15).

7) Martensite plates do not generally grow across grain boundaries (6,16). The advancing plate is stopped at parent phase grain boundaries and by other plates. Therefore, the martensite grain size is smaller than that of its parent phase.

8) Many martensites are "crystallographically" reversible by heating, but with considerable hysteresis (16). The reverse reaction is believed to take place by shear similar but opposite in sign- to the reaction on cooling. However, not all martensites are practically reversible due to their decomposing into more stable products on heating.

9) "Athermal" martensites, especially typical of iron-based alloys, are unique in that they form only during cooling. Here the temperature at which martensite starts to transform (M_s) is independent of cooling rate as long as it is above a critical minimum. However, isothermal martensite in which M_s is suppressed with increasing cooling rate and in which transformations proceed at a given temperature below M_s also occur (21,22,23,24).

Two types of athermal martensite exist: the first, typical of iron-nickel alloys (25), is formed by new plates which shoot out to their final size in one burst; the second, exemplified by the Au Cd system, forms in a series of propagating steps (26).

10) When athermal martensites are forming, interruption of cooling in the martensite range halts the transformation, which resumes at a temperature, M_s', below the holding temperature when cooling is continued. This phenomenon is known as stabilization (27).

The reverse of stabilization can occur in some alloy steels when they are held at a temperature above M_s. In this case, M_s' is higher than M_s and the phenomenon is called "conditioning" (16).

11) Iron-based martensites will decompose to the equilibrium products on heating and are thus considered a metastable state between the parent and equilibrium phases (28).

12) Martensite may be a non-equilibrium phase but is not necessarily so, for example in pure metals (46).

13) Alloy compositions generally dictate the M_s temperature, which is usually lowered with increasing solute content (17,18,20,29,30).

14) Martensitic reactions are strain-sensitive and can be made to occur at temperatures above M_s (ie, M_s is increased) by means of plastic deformation. Strain sensitivity decreases with increasing temperatures in such a way that there is a limiting temperature (M_d) above which martensite will not form (16,31,32,33).

15) The M_s temperature of iron-based martensites can be depressed by applying high hydrostatic pressure to the transforming specimen (3,4).

16) Martensite "needles" or "plates" are generally ellipsoidal or lenticular as a result of opposing stress-fields imposed by the surrounding matrix (8).

17) The hardness resulting from stress in the parent matrix in iron-carbon martensites is not

typical of all martensites (35).

The "surface rumpling" criterion for the recognition of martensite does not remain unchallenged (44). It has been shown that some diffusion controlled reactions may exhibit a similar phenomenon. Also, this criterion cannot differentiate between surface martensite and bulk martensite. When Yeo's work (52) was repeated using electrical resistivity measurements, it was shown that the structure identified as martensite on the basis of surface rumpling was in fact only a surface phenomenon.

In summary, beyond the statement that the martensitic process is characterized by a cooperative movement of atoms resulting in a new phase, a definitive and inclusive definition of martensite cannot be given (46). However, the surface rumpling criterion remains the most useful criterion in the recognition of martensite and is a valuable tool when applied with caution.

III--The Massive Transformation

In 1939, Greninger (36) coined the term "mass transformation" to describe the reaction that he observed in rapidly cooled Cu-9.3% Al alloys. Previously, similar reactions were observed by Mehl and Smith in 1934 (37) and by Phillips in 1930 (38). This reaction has been studied in several alloy systems and it has been widely accepted that, although closely associated, the massive and martensitic transformations are distinct (39,40). Unfortunately, confusion has developed over the terminology involved in classifying the structural variants. Further, the factors which control the structural variations on quenching have not been completely elucidated and a consistent and general explanation of structural characteristics as a function of solute type and content has not yet been accomplished (20).

The structure that Massalski (40) calls "massive" exhibits the following properties:

1) There is no bulk charge in the composition from that of the high temperature parent phase (41,42). In this respect massive and martensitic structures are similar.

2) The massive structure displays a jagged boundary composed of many planar segments when it is present in a matrix of some other constituent.

3) If the structure is solely "massive", the massive grains may extend across previously existing

grain boundaries of the parent phase. Further, the grain boundaries may appear straight on many sides (43) or may be smoothly curved (40).

4) A strict crystallographic relationship does not exist between the massive and parent structures although a limited correlation may exist (40,42).

5) No shape change (ie, no surface rumpling) accompanies the massive transformation (43,39).

In addition to the above common features, the following features have been associated with massive transformations:

1) Massive transformations occur at cooling rates less severe than required for martensitic transformations and can usually be depressed by rapid cooling. This feature suggests a thermally activated process (11,39).

2) Both massive and martensitic structures may occur in the same alloy depending on the cooling rate (17,28,47,48). In this case, more rapid cooling suppresses the massive transformation in favour of the martensitic process.

3) Massive and martensitic transformations do not take place in the same temperature range. The characteristic temperature for the massive transformation is higher than the M_s temperature (39,40). It has been suggested by Owen (39)

that this feature indicates a lower driving force for the massive reaction than for the martensitic reaction.

4) The speed of the massive reaction is two orders of magnitude greater than that of a diffusion process producing equilibrium products. In this connection, the major part of the transformation occurs as a propagation of incoherent boundaries of the massive phase in a manner expected of a diffusion-controlled process (42).

5) Sub-grain networks are often associated with massive structures (50).

6) On transformation, the massive product nucleates at grain boundaries of the parent phase and the growing products are incoherent with the surrounding matrix (10).

There has been some discussion and disagreement in the literature as to the mechanism involved in massive transformations. However, Massalski presents a strong case for a short range diffusion process. He and his co-workers (10,40) have shown by X-Ray and optical metallography that growing massive crystals cross grain boundaries of the high temperature parent phase and that little, if any, crystallographic relationship exists between orientations of parent and product phased. Further Massalski and Kettl (42) have shown by means of

a cinefilm that the massive phase interface propagates discontinuously with time and leaves a shear-like trace behind. In addition, it has been shown that the massive transformation can be suppressed in favour of a martensite reaction at high quenching rate (47,48). These observations suggest a thermally activated diffusion process. However, the lack of bulk diffusion and the cooling rates involved would exclude any type of long range or even intermediate range diffusion phenomena. It therefore seems more likely that the movement of individual atoms is restricted to a few interatomic distances. Thus a mechanism of short range diffusion across an incoherent or semi-coherent interface has been adopted by many investigators (10,11,39,40,41,42 50). In addition, Christian, Wayman and Reed (11) suggest that, in some cases, the massive structure may nucleate in a partially coherent manner and then grow by short range diffusion in an incoherent manner.

IV--MASSIVE MARTENSITE

Owen and Wilson (51) have asserted that a second form of massive reaction in addition to the short range diffusion type may occur in some alloys. They use the term "massive martensitic" to describe the structure since it is believed that it forms martensitically (51, 53). There is considerable doubt as to the validity of the distinction between conventional martensite (sometimes referred to as "acicular" (30,49))and "massive martensite". The structure that is referred to as "massive martensite" exhibits the following characteristics:

1) Grains of the product phase do not cross the original boundaries of the high temperature parent phase.

2) Surface relief effects are present due to parellel arrangements of shear plates or laths within the metal.

3) In general, the interfaces between grains are similar to those in a purely massive structure.

Yeo (52) has demonstrated that a habit plane is associated with the massive structure and Saburi and Wayman (41) have established that lattice correlations exist between the parent phase and the transformed product.

Marder and Kraus (30) have used transmission electron microscopy to study "acicular" and "massive" martensites in dilute iron alloys and have demonstrated a morphology

difference between the two. They made the following observations:

1) Massive-martensite in dilute iron-carbon alloys is composed of packets of parallel laths or plates in contrast to the acicular structure found in more concentrated alloys, which were composed of irrationally arranged plates in a matrix of austenite.

2) The aligned laths of a packet of massive martensite are in a limited number of orientations and are not possible in a b.c.c. twinning relationship.

3) A transition in morphology from massive to acicular martensite occurs in the range of carbon contents from 0.6% to 1.0% by weight. Below 0.6%C, the structure is massive and above 1.0%C, the structure is acicular.

However, the use of the term "massive-martensite" leads to some confusion with the massive transformation that occurs by diffusional nucleation and growth. The term is, perhaps, unnecessary, because it is applied to a special form of martensite in which the subtle differences between it and conventional martensites have been conclusively revealed by electron-microscopy only in a limited number of cases. Further criticism of the term arises from Marder and Kraus' third observation, ie, that the morphological change occurs in the range

of 0.6 to 1.0 wt % carbon in Fe-C alloys. Studies of the M_s temperature of iron-carbon alloys over a range of compositions from 0.2% to 1.4% carbon show a steadily decreasing M_s temperature as the carbon content increases (9,12,18,25). When M_s is shown as a function of carbon content, no change is observed over the range of 0.6 to 1.4% carbon that can be attributed to a change in mechanism. Further, when the degree of tetragonality in the structure of iron-carbon martensite (determined by X-ray diffraction) is shown as a function of carbon content over the range 0.55 to 1.8% carbon, the function is linear and decreases with decreasing carbon content over the entire range, with no signs of a structure change attributable to a change in mechanism (53,54). For these reasons, the remainder of this thesis will not distinguish between the two types of martensite.

V--MASSIVE AND MARTENSITIC TRANSFORMATIONS IN IRON

The iron-carbon system has remained the backbone of commercial heat-treatable steels for decades. It was in this system that martensite was first discovered and, although the structure itself is not used commercially, an understanding of it is essential because it is the first step in the production of the tempered (or precipitated) structure that accounts for much of the importance of alloys based on the iron-carbon system. In addition, it is reasonable to suggest that an understanding of the martensitic reaction in iron alloys and pure iron may lead to a better understanding of the martensitic transformation in general.

Face-centred-cubic (γ) iron will accept carbon as an interstitial solute up to 2%; but carbon is relatively insoluble in body-centred-cubic (α) iron. When γ-iron is slowly cooled, the carbon present diffuses out of solution to form iron-carbide (Fe_3C) as the γ-iron transforms to α-iron. Rapid cooling of γ-iron decreases atomic mobility such that the formation of Fe_3C is suppressed and carbon remains in solid solution at room temperature, with the result that the cubic lattice distorts to produce the body-centred-tetragonal structure associated with iron-carbon martensite. It has been shown that decreasing the carbon content reduces the degree of tetragonality (54). The axial ratio of an

iron-carbon martensite containing 1.4% C is 1.068 while pure iron martensite is cubic (53,54). It has also been shown that as the carbon decreases, the M_s temperature increases (18) (Figure 1).

The measurement of the M_s temperature in pure iron has attracted considerable attention in the literature and is ranked with some importance since a final agreement on its value would help in interpreting the relative merits of existing theories about the thermodynamics of the martensite reaction. However, final agreement has not yet been established. Data from the iron-carbon system previous to Bibby and Parr's work (18) extrapolated to 520°C, while data from iron-nickel and iron manganese extrapolated to 747°C (55). Swanson and Parr (17) show iron-nickel data extrapolating to 680°C.

Measurements of the M_s temperature in pure iron previous to Bibby and Parr were made by Esser et al (74), Duwez (62) Gilbert and Owen (39) and Srivastava and Parr (63). Table 2 from Bibby and Parr summarizes the M_s values obtained, the cooling rates at which transformation occurred and the purity of the iron in investigations prior to their own. In reference to this table, the following observations are made:

i) the expressed composition of the iron is not inevitably correct. Carbon analyses at low values are not always reliable and the bar compositions

may not be typical of the sample used in the experiment because of local segregation effects.

ii) There is no record of martensite formation being confirmed by metallographic examination for a shape change in any of the work quoted other than that of Srivastava and Parr.

Bibby and Parr established 750°C as the M_s temperature for iron containing no more than 0.0017% carbon by weight (plus 0.0015% metallics) and demonstrated that the M_s temperature and the critical cooling rate required to obtain martensite are extremely sensitive to even very small changes in carbon content. The M_s of 750°C obtained at a critical rate of 35,000°C fell to 540°C at a critical rate of 5000°C/sec with only a small increase in the carbon content. At intermediate rates (less than the critical rates), a massive structure was observed to form at temperatures above the measured M_s a phenomenon that has also been reported by Pascover and Radcliffe (56).

Beyond giving the M_s of 750°C for iron containing 0.0017%C, Bibby and Parr could only suggest a qualitative description of the effects of carbon on the M_s temperature and critical cooling rates in very dilute iron-carbon alloys since the exact carbon content of their small samples carburized in the gas quenching apparatus could not be determined accurately. As a result, their conclusions were tentative.

In a related series of investigations, Parr and his co-workers investigated the effects of carbide forming elements (manganese and chromium) and of non-carbide forming elements (nickel and cobalt) in binary alloys with iron (plus the inevitable melt quantities of carbon) in an effort to clarify the effects of small quantities of carbon on the M_s temperature. The results of these investigations are summarized below:

1) Iron-Nickel (Swanson and Parr (17)): Iron-nickel alloys were investigated and massive and martensitic structures were reported with transformations versus cooling rate curves similar to Bibby's curves for iron-0.0017% carbon. The iron used in this study contained 90 ppm carbon and a M_s of 680°C for Fe-0% Ni (+90ppm Carbon) was reported.

2) Iron-Cobalt (Parr (19)): Iron-cobalt alloys were subjected to high rates of cooling and displayed massive and martensitic transformations similar to those reported by Bibby and Parr. For alloys containing less than 0.57%Co, the M_s for pure iron extrapolates to about 740°C which agrees well with Bibby and Parr's work.

3) Iron-Manganese (Gomersall and Parr (43)): The results from the iron-manganese were inconclusive in that no clear separation in

transition mode with increasing quenching rate could be detected.

4) Iron-Chromium (Wallbridge and Parr (44)): The results from the iron-chromium alloys were very similar to those of the iron-manganese alloys and, likewise, the results were inconclusive.

In reference to the iron-nickel alloys, Yeo (52) reports a sharp increase in the transformation temperature with decreasing carbon content and suggests that carbon free alloys be investigated in order to reassess the theories of the martensitic transformation.

In summary, the carbide forming alloying elements failed to give results that could help to clarify the roll of carbon in martensite, and the results of Bibby and Parr remain qualitative rather than quantitative. Further, their results are not without some detracting opinion. Pascover and Radcliffe (56) report an M_s for pure iron, based on extrapolation from iron-chromium data, of 700°C and use a thermodynamic approach to support their result. For these reasons, the present investigation was undertaken to establish a quantitative relationship between the M_s, the critical cooling rate and the carbon content in very dilute iron-carbon alloys.

EXPERIMENTAL

I--Gas Quenching

The cooling rate data used in the investigation were obtained by use of a high velocity gas quenching apparatus shown in Figure 2.

The design of the unit is based on the original by Greninger (61) and the modified designs by Duwez (62) Srivastava (63) and Bibby (58).

The essential features of the gas quenching apparatus used in the present work are:

(a) a high vacuum system to avoid atmospheric contamination,

(b) a resistance furnace using a tungsten heating element,

(c) a quenching jet fed by hydrogen, helium or argon,

(d) a means of holding the sample,

(e) an oscilloscope to record the cooling curves.

The vacuum system consists of a Cenco mechanical pump and a two inch Edwards Speedivac mercury diffusion pump with a liquid nitrogen vapour trap, to evacuate a twelve inch bell jar. A General Electric hot cathode ionization gauge, type 22 GT 103, is used to measure the pressure of the system.

The quench unit comprises a twelve inch bell jar sealed by an "L"-ring on a finely machined stainless steel

plate which has vacuum outlets to the gas quenching jet, to the ionization gauge and to a rough vacuum by-pass line. The plate is connected to the high-vacuum pumping system by a two-inch Speedivac valve.

Vacuum-sealed current terminals are used to supply power to the heating coil and to introduce the thermocouple leads to the system. These, as are all the openings into the system with the exception of the ionization gauge, are sealed by means of nitrile "O" rings. (The ionization gauge is sealed with an annealed copper vacuum seal).

The specimen is held inside the heating coil by means of the thermocouple leads and an alumina thermocouple sheath, which is held by a cross-bar and pillar as illustrated in Figure 3.

The heating coil consists of one turn of 0.020" diameter tungsten wire and is powered by a 250 VA-115 volt primary--7.5 volt secondary variable transformer, which is controlled by a 0-140 volt variac.

The quenching jet consists of a Laval-type convergent-divergent nozzle situated directly beneath the specimen. An Asco type NPT - 8210C solenoid valve is mounted directly beneath the jet and is connected to a regulated high pressure gas bottle by means of ½ inch pressure line. The type of gas used (hydrogen, helium and argon) and the regulated pressure are varied according to the desired quenching rates. The maximum

cooling rates are obtained using hydrogen at 100 psi.

The solenoid is powered by a 110 volt source through a switch that simultaneously turns the heating coil off and opens the solenoid.

A heat shield is not used around the jet since quenching rates up to 115,000°C/sec can be obtained without one.

A Tektronix 564 storage oscilloscope with a type 3A3 differential amplifier and a type 2B67 time base was used to record the cooling curves. This unit has a voltage range from 0.1mv/cm to 10 mv/cm (± 3%) and a time base range of 1 u sec/cm to 5 sec/cm (± 3%). The rise time on this combination is 0.7 u sec.

A Leeds and Northrup millivolt potentiometer was used to calibrate the voltage scale of the oscilloscope. The cold junction used was room temperature as measured by a thermometer accurate to ± 1°C.

II--Samples

The samples were prepared from a two inch diameter bar of high purity iron supplied by Battelle Memorial Institute (see ingot analysis, Appendix II) by cutting and rolling into strips 6" x 2" x 0.010". Carbon pick up during these operations was estimated to bring the carbon content to 10 ppm. The samples were carburized in an atmosphere of flowing methane at 870°C and then decarburized in "wet" hydrogen at 925°C to the desired

carbon content. The samples were then sealed in quartz under an argon atmosphere and homogenized for 30 hours at 1050°C. Appendix I contains a complete description of the alloy preparation.

After homogenization, part of each sample was sent to Battelle Memorial Institute to be analyzed by the method described in Appendix III.

The remaining parts of each sample were thinned by electro-polishing to a final thickness of 0.002 inches in an electrolyte consisting of 90% glacial acetic acid (99.5% pure) and 10% perchloric acid (concentration, 70% by weight) between two large mild steel electrodes. The electrolyte was constantly stirred and power was supplied by an Electro Model D-612T power supply. The best results were obtained with a potential of 15 volts and a current density of 0.3 amperes per square inch of sample surface producing a polishing rate of 0.003 in/hr.

Specimens for quenching were prepared from the resulting foil by spot welding a small amount of the material around a thermocouple junction fabricated from 0.004 inch diameter chromel-alumel thermocouple wire. Care was taken to keep the welding current at the lowest values consistent with good welds in order to minimize any possible contamination of the specimens. Each specimen was trimmed to a final size of about one half millimeter square before quenching.

III--Quenching Method

The gas quenching unit was first outgassed by evacuating the bell jar to a pressure of 10^{-5} Torr and heating the furnace element to red heat.

When the specimen was placed in the unit, the system was evacuated to 10^{-5} Torr, back filled with either helium or hydrogen and evacuated again to a pressure in the range 5×10^{-6} to 10^{-5} Torr. The specimen was heated to 965°C for about one minute and then quenched.

A check was kept on the oscilloscope calibration by means of the potentiometer during testing to ensure that it did not drift out of calibration.

A Polaroid Land Camera was used to photograph the trace from the face of the storage tube. A typical curve is shown in Figure 4.

Various quenching rates from 100°C/sec to 115,000° C/sec can be obtained with this apparatus by varying the type of gas (hydrogen, helium and argon were used), the regulated pressure of the gas (0-100 psi), the position of the sample and the size of the sample. Although the size parameter is not an appealing variable due to possible size effects on the transformations, tests on specimens over the range of sizes used showed no noticeable change in the results.

RESULTS

Figures 5-9 indicate the effects of cooling rates on the transformation temperatures of the iron carbon alloys in the composition range 15-187 ppm by weight of carbon. The general form of the curves is similar: with increasing cooling rate, the transformation temperature decreases substantially until a critical minimum cooling rate in the range 4,000-10,000°C/sec is achieved. There is no further decrease in the transformation temperature until a second critical cooling rate in the range 10,000-32,000°C/sec is reached, after which the transformation temperature decreases to a second "plateau" where it remains constant as the cooling rate is further increased to the maximum attainable.

Metallographic examination of specimens polished before they were transformed indicates that the first, or higher plateau represents the $\gamma \rightarrow$ Massive transformation temperature and that the second, or lower, plateau represents the $\gamma \rightarrow$ Martensite transformation temperature (M_s). Figures 10-12 are micrographs of the prepolished specimens after transformation. The massive samples (Figure 8) consist of an equiaxed structure with 120° grain boundaries and no surface rumpling. The martensitic samples display the surface rumpling characteristic of martensite.

Figure 13 is a summary of Figures 5-9 and shows, with increasing carbon content, a decrease in the $\gamma \rightarrow$ Massive and $\gamma \rightarrow$ Martensite transformation temperatures and a decrease in the minimum cooling rate required to get the massive and martensitic structures. These trends are further illustrated in Figures 14 and 15.

It should be noted that the decrease from the massive to the martensite transformation temperatures with increasing cooling rate could be followed with a fair degree of certainty for the two highest carbon contents (187 and 143 ppm). For the other samples, however, the scatter of the results in the region was such that the temperature transition from one plateau to the other could not be followed.

Attempts were made to establish a curve for iron-6ppm carbon, but, as yet, reproduceable results have not been obtained. Results obtained show a scatter of transformation temperatures in the range of 725-800°C, which could not be reproduced at any given cooling rate.

The effects of changes in specimen size within the limits of the procedure (representing a volume change of 200x) had no effect on the transformation temperature for a given carbon content at a given cooling rate. Also, varying the soaking time at 965°C from less than 10 seconds to 5 minutes had no effect so long

as the vacuum was maintained at 10^{-5} Torr or better.

The pressure inside the quenching apparatus had a very great effect on the results. Reproduceable data could not be obtained if the pressure during soaking was greater than 3×10^{-5} Torr. As the carbon content was decreased, the sensitivety to the vacuum seemed to increase. The most consistent results were obtained when the chamber was evacuated to 10^{-5} Torr, backfilled with hydrogen or helium and evacuated again to a pressure below 10^{-5} Torr.

DISCUSSION

The present investigation has produced results that form a more complete picture of the transformation rate data in dilute iron carbon alloys. They are in very good agreement, where comparable, with those of Bibby and Parr (58) (M_s - 750°C for Fe-17 ppm C versus M_s = 750°C for Fe-15 ppm C for the present results), but differ from the M_s for iron-90 ppm carbon reported by Swanson and Parr (17) (680°C versus 625°C in the present results, as taken from Figure 14). However, the present investigation surveyed a range of carbon contents using samples all made from the same ingot of high purity iron, the analysis of which was accurately determined (Appendix II). A total of almost 500 transformations were measured to study the single parameter of carbon content to nullify any possible effect due to local segregation effects. Care was taken to introduce no other possible parameters such as contamination due to inadequate vacuum during quenching.

The results are not in agreement with those reported by Pascover and Radcliffe (56) (they report M_s= 700°C for pure iron based on data from the iron chromium system). However, in the present study it was determined that a vacuum within the quenching apparatus had a very large effect on the transformation.

Pascover and Radcliffe report that they employed a vacuum of 10^{-4} Torr while the present investigation showed that a vacuum of 10^{-5} Torr or better is necessary to assure reproduceable results.

Pascover and Radcliffe used a thermodynamic approach to support their data--an approach that is not without valid criticsm.

The thermodynamics of the martensite transformation do not permit a rationalisation of the discontinuity in the relationship between M_s and the carbon content that Bibby and Parr reported, and which is put into quantitative terms by the current investigation.

The difficulties involved in handling the quantum mechanical approach to transformations in solids have caused many investigators to be attracted to a thermodynamic approach. Such an approach has been taken, for example, by Cohen, Macklin and Paranjpe (16). They combine thermodynamics and various physical phenomena in order to deduce a free energy change for the γ-iron $\rightarrow$ martensite reaction. Following their approach, a free energy decrease, $F_\gamma - F_m > 0$, accompanies the γ-iron $\rightarrow$ martensite reaction. Considering a two step process,

$$\gamma\text{- iron} \rightarrow \alpha\text{-iron} \rightarrow \text{martensite},$$

on a one mole basis,

$$F_m - F_\gamma = (F_\alpha - F_\gamma) + (F_m - F_\alpha) \qquad (1)$$

where:

F = molar free energy

α represents b.c.c. iron (ferrite),

γ represents f.c.c. iron (austenite),

and

m represents martensite (b.c.t.).

Now, where N_{Fe}, N_C and N_j are the mole fractions of iron, carbon and each of the additional alloying elements respectively, and u is the corresponding chemical potential,

$$F_\alpha - F_\gamma = \left[(N_{Fe}u_{Fe})_\alpha + (N_C u_C)_\alpha + (N_j u_j)_\alpha\right] - \left[(N_{Fe}u_{Fe})_\gamma + (N_C u_C)_\gamma + (N_j u_j)_\gamma\right]. \quad (2)$$

The standard states are taken as pure b.c.c. iron, pure f.c.c. iron and pure graphite. When no alloying elements other than carbon are present, the j terms in equation (2) disappear. Thus, rewriting equation (2) for the standard states, assuming $N_j = 0$,

$$F_{o\alpha} - F_{o\gamma} = \left[(N_{Fe}u_{Fe})_{o\alpha} + (N_C u_C)_{o\alpha}\right] - \left[(N_{Fe}u_{Fe})_{o\gamma} + (N_C u_C)_{o\gamma}\right]. \quad (3)$$

Therefore, subtracting equation (3) from equation (2) and noting that $(u_i - u_i^o) = RT \ln a_i$ where a_i is the activety of component i in a given phase:

$$F_\alpha - F_\gamma = N_{Fe}\left[(u_{Fe})_{o\alpha} - (u_{Fe})_{o\gamma}\right] + N_{Fe}RT \ln\left[\frac{(a_{Fe})_\alpha}{(a_{Fe})_\gamma}\right] + N_C RT \ln\left[\frac{(a_C)_\alpha}{(a_C)_\gamma}\right] \quad (4)$$

The term $(u_{Fe})_{o\alpha} - (u_{Fe})_{o\gamma}$ can be obtained from the data of Darken and Smith (63) and the carbon activities for the third term in equation (4) come from Smith's work (65). The iron activities are obtained on a linear extrapolation of ln a_c versus $\frac{1}{T}$ (the Gibbs-Duhem equation).

The remaining term in equation (1), $(F_m - F_\alpha)$, is assumed to arise entirely through the tetragonality of the lattice and is given as

$$F_m - F_\alpha = \tfrac{1}{2} V_m (\sigma_x \varepsilon_x + \sigma_y \varepsilon_y + \sigma_z \varepsilon_z) \qquad (5)$$

where:

V_m = volume per mole of martensite

σ = principal stresses

ε = principal strains.

The principal stresses are calculated from the strains and the elastic constants (Young's modulus and Poisson's ratios; $E = 30 \times 10^6$ psi and $\mu = 0.3$) and the principal strains are taken from lattice parameter measurements.

Hence, by this approach, the free energy change $F_m - F_\gamma$ can be calculated as a function of temperature. Cohen et al (16) evaluated equation (4) for carbon concentrations between 0% and 1.2% and found that the M_s values always lie a distance of 290 cal/mole below the equilibrium free energy temperature (ie, below the temperature at which $F_\gamma = F_\alpha$). Thus, they assumed that all iron-carbon martensites in the composition range 0%-1.2% carbon require a driving force of 290 cal/mole.

The non-chemical contributions to the martensite reaction were estimated to be 65 cal/mole which led to the suggestion that there exists a barrier to the transformation. Otherwise, the reaction would begin at a driving force of 65 cal/mole.

In reviewing the thermodynamic approach, Bibby (58) and Bibby and Parr (18) made the following observations:

1) Since martensite is not an equilibrium phase, treatment by classical thermodynamics is questionable.

2) It is implied in the theory that the height of the free energy barrier is 290 cal/mole. Yet it is the quantity $F_\gamma - F_m$ that has been calculated to be 290 cal/mole.

3) In the expression $F_m - F_\gamma = (F_\alpha - F_\gamma) + (F_m - F_\alpha)$, the $F_m - F_\alpha$ term arises only through tetragonality induced by the carbon atoms. This term in pure iron is zero since pure iron is cubic.

Therefore:

$$F_m - F_\gamma = F_\alpha - F_\gamma$$

$$F_m = F_\alpha$$

However, Singh and Parr (48) have shown that the free energy of ferrite is not the same as that of martensitic pure iron. Hence the assumption that the $F_m - F_\alpha$ term is solely ascribably to tetragonality induced by carbon appears to be in error.

In addition to Bibby and Parr's observations, the following shortcomings of the thermodynamic approach are suggested:

1) It does not consider the effects of any possible change in reaction mechanism. That is, it assumes the required driving force is independent of the reaction path--an assumption that is not necessarily valid.

2) No consideration is given to the changes in the thermodynamic functions occurring at the Curie point of iron (770°C) that were reported by Cody et al (68) and by Anderson and Hultgren (67). Both of these investigations showed pronounced variations in the thermodynamic functions near the Curie point and the α to γ phase transformation temperature, a range which is important when considering the martensite reaction.

In light of the deficiencies of the thermodynamic approach to the martensite transformation, the effects of small amounts of carbon will be appraised in relationship to the new data supplied by the present investigation.

There is a notably close agreement between the carbon content at which the M_s starts to sharply increase with decreasing carbon content and the solubility limit of

carbon in α-iron. Esser's point in Figure 1 depicts an M_s temperature of 520°C at a carbon content of 170 ppm and marks the approximate beginning of the upswing of the M_s temperature. The solubility limit of carbon in α-iron is 180 ppm at 720°C (the eutectoid temperature) (69).

The solubility limit of carbon in α-iron at 720°C indicates that one carbon atom is to be found in every 600 α-iron unit cells (or one carbon atom per 1200 iron atoms), assuming random distribution (69). Thus, it can be seen that carbon has a long range effect on the lattice of b.c.c. iron: that is, the effect of a single carbon atom extends beyond the unit cell. One carbon atom per 600 unit cells in b.c.c. iron corresponds to an individual carbon atom's having a sphere of influence of about 6 atomic distances. This is comparable to the field distortions of lattices due to dislocations (70).

The extent of the variation in the lattice parameters in martensite as a function of carbon content has been determined by Roberts (54) and Kurdjumov (7), who are in close agreement. From their data:

$$c = b + 0.117\ d$$

and

$$a = b - 0.014\ d$$

where

b = cell dimension

d = weight percent carbon,

c and a are the cell dimensions of the tetragonal lattice.

The rate of extension of c, (0.117 d), is an order of magnitude greater than the rate of contraction of a, (0.014 d). In a two dimensional representation of the iron array, with one carbon atom in an interstitial position, as shown in Figure 16, the carbon atom tends to repel the iron atoms on either side of it, thereby distorting the lattice and increasing its energy. Now, considering the case where a second carbon atom is in a neighbouring site, as shown in Figure 17, the energy of the lattice is again increased, but the increase will not be as great as that caused by the first atom. In general, any carbon atom with a field of influence overlapping that of the first atom will cause an increase in lattice energy less than that caused by the first carbon atom. Therefore, where there is a homogeneous distribution of carbon atoms, the lattice energy will increase rapidly until the spheres of influence of individual carbon atoms begin to overlap and then the energy increase will occur at a lower rate as further carbon is introduced to the lattice.

It seems reasonable to assume that the sphere of influence of a carbon atom in the b.c.t. structure is the same as in the b.c.c. at the eutectoid temperature (6 atomic distances) because the formation of

martensite involves quenching the sample through the eutectoid temperature. Hence, the greatest energy change, as a function of carbon content, would take place in the carbon range of 0 - 180 ppm and smaller energy changes would be associated with carbon contents greater than 180 ppm. Consequently, one would expect the M_s temperature to fall very quickly with carbon additions in the 0 - 180 ppm range and less quickly above 180 ppm. There is, of course, a decrease in the solubility limit of carbon in α-iron as the temperature falls from 720°C to 520°C (ie, from the eutectoid temperature to the M_s temperature of iron containing 180 ppm C); but the decrease is small and is probably overshadowed by an inevitable non-homogeneity of carbon distribution.

A second consideration arises from an examination of Figure 14. This diagram shows that the M_s temperature increases more rapidly with decreasing carbon content than does the massive transformation temperature. If the two curves are extrapolated to lower carbon levels, they meet at a temperature of 770°C and a carbon content of 5 - 6 ppm. In consideration of the approximate nature of the curves, they are unlikely to intersect at a positive carbon value since this would indicate an M_s temperature higher than the massive transformation temperature at lower carbon levels - a most impossible situation.

A rationalization for the curves of M_s temperature and massive temperatures versus carbon content meeting at a carbon content greater than 0 ppm has been offered by Smith (71) and by Maringer et al (72) who found evidence that some carbon present in iron is trapped at vacancy sites. Maringer found evidence from internal friction studies, magnetic measurements and total carbon analysis that about 6 ppm carbon are associated with vacancies at 700°C. Although Maringer concluded that the amount of carbon associated with vacancies is temperature dependent, his work did not extend above 850°C. Further, in an unrelated investigation, Falquero (73) found indirect evidence of similar carbon-vacancy reactions in iron above 910°C. In addition, it is thermodynamically probable that some carbon would be tied up in vacancy sites and therefore unavailable to affect the transformation.

If this extrapolation is valid, two alternate cases may exist:

1) The M_s and massive transformation temperatures are the same in "pure" iron (ie, iron in which all carbon occupies vacancies).

2) There is no martensitic transformation in "pure" iron; that is, only massive transformation takes place.

The second alternative does not appear to be attractive when Figure 15 is examined. This figure indicates a

reduction in the rate of increase of the critical cooling rate with decreasing carbon content, and would extrapolate to a value of about 47,000°C/sec at 0 ppm carbon. In this regard, it should be borne in mind that the present investigation did not provide reproduceable results with an iron-carbon sample containing 6 ppm carbon.

The temperature at which the M_s and massive temperature curves meet is 770°C - the Curie temperature of pure iron. It seems unlikely that this should be considered a coincidence as it brings to mind Zener's (1,3) considerations on the $\gamma \rightarrow \alpha$ transformation discussed in the general introduction. However, an evaluation of the quantum physics involved in Zener's work is beyond the scope of the present thesis. Further, it would be unwise to develop a hypothesis until data for a 6 ppm carbon alloy are developed.

CONCLUSIONS

1) The present investigation has established 750°C as the M_s temperature of iron containing 15 ppm carbon and puts the qualitative observations of Bibby and Parr (18) regarding the sensitivity of the M_s temperatures to small increases in carbon content into quantitative terms, as illustrated in Figure 14.

2) When the M_s and massive temperatures are plotted as functions of carbon content (Figure 14), they meet at 770°C and 6 ppm carbon - if the extrapolation is to be accepted in the absence of data for a 6 ppm sample. If the extrapolation is valid, the Curie temperature and the M_s temperature of "pure" iron coincide.

3) The discontinuity in the plot of the M_s temperature versus carbon content presented in Figure 1 and confirmed by the present investigation suggests the likelihood of a change in the mechanism of the martensitic transformation over the composition range of 0-180 ppm of carbon - that is to say, the mechanisms involved in the formation of pure-iron martensite and iron-carbon martensite (carbon content > 180 ppm) are different.

4) The likelihood of there being no martensitic reaction in pure iron - ie, that the reaction is purely massive at all quenching rates-is discounted since Figure 14 strongly suggests a critical quenching

rate of 47,000°C/sec to obtain martensite in pure iron.

In light of the above conclusions, the following suggestions for further work are put forward:

1) Further attempts to obtain data for the M_s and massive temperatures for a 6 ppm sample should be made.

2) A detailed study of the martensitic and massive reactions in iron-carbon alloys over the carbon range of 0-300 ppm employing electron microscopic and micro-beam X-ray techniques should be undertaken to investigate the morphology and the possible change in mechanism of the martensitic reaction.

3) A study parallel to the present investigation using the iron-nitrogen system at very low nitrogen contents could be valuable as Owen and Bell (49) have pointed out the similarities between the iron-carbon and iron-nitrogen systems.

REFERENCES

1. Zener, C. Physics Rev. 71 (1947) p. 846
2. Kaufman, L., Clougherty, E.V. and Weiss, R.J. Acts Met II (1963) p. 323
3. Zener, C., Trans. AIME 203 (1955) p. 619
4. Hume-Rothery, W. The Structure of Alloys of Iron, (Pergamon Press, London, England 1966) p. 6
5. Zackay, U.F. (et.al.) "Strengthening by Martensite Transformations" in Strengthening Mechanisms in Solids (ASM, Metals Park, Ohio, 1960)
6. Hume-Rothery, W. ibid, p. 226 and 229
7. Kurdjumov, C.U. JISI 195 (1960) pp. 26-48
8. Bilby, B.A. and Christian, J.W. Inst. of Metals Monograph and Report Series No. 18 (1956) p. 121
9. Greninger, A.B. and Troiano, A.R. Met. Prog. 50 (1946) p. 303
10. Christian, J.W. The Theory of Transformations in Metals and Alloys (Pergamon Press, London, England 1965) p. 803
11. Christian, J.W., Read, T.A. and Wayman, C.M., Crystallographic Transformations in Intermetallic Compounds (ed. Westbrook, J) (John Wiley & Sons, Inc. New York, 1967)
12. Greninger, A.B. and Troiano, A.R. Met. Prog. 185 (1949) p. 590
13. Bunshah, R.F. and Mehl, R.F. Trans. AIME 197 (1953) p. 1251

14. Kulin, S.A. and Cohen, M. Trans ASM 41 (1949) p. 1024

15. Macklin, E.S. and Cohen, M. Trans AIME 191 (1951) p. 746

16. Cohen, M., Macklin, E.S. and Paranjpe, U.G., "Thermodynamics of the Martensite Reaction" in Thermodynamics in Physical Metallergy (ASM, Metals Park, Ohio, 1952) p. 242

17. Swanson, W.D. and Parr, J.G. JISI 202 (1964) p. 104

18. Bibby, J., and Parr, J.G., JISI 202 (1964) p. 100

19. Parr. J.G., JISI, 205 (1967) p. 426

20. Pascover, J.S. and Radcliffe, S.V. Trans. AIME 242 (1968) p. 673

21. Averback, B.L. and Cohen, M., Trans ASM 41 (1949) p. 1024

22. Kurdjumov, G.U. and Masksimoua, O.P. Dohl Akad, Nauk, SSSR 61 (1948) p. 83

23. Kurdjumov, G.U. and Masksimoua, O.P. Dohl Akad Nauk, SSSR 73 (1950) p. 95

24. Kurdjumov, G.U. and Masksimoua, O.P. Dohl Akad Nauk, SSSR 81 (1951) p. 565

25. Kaufman, L. and Cohen, M., Journal of Metals 8 (1958) p. 1393

26. Lieberman, D.S., The Mechanism of Phase Transformations in Metals, Inst. of Metals Monograph and Report Series No. 18 (1955), Discussion

27. Harris, W.J. and Cohen, M., Trans. AIME 185 (1949) p. 447

28. Barrett, C.S., Structure of Metals, (McGraw Hill Publishing Co. New York, 1952 p. 559

29. Snape, S. and Schaller, F.W. Trans AIME 61 (1968) p. 631

30. Marder, A.R. and Kraus, G. Trans ASM 60 (1967) p. 651

31. Kulin, A., Cohen, M. and Averback, B.L. Trans. AIME 4 (1952) p. 661

32. Troiano, A.R., and McGuire, F.T., Trans. ASM 31 (1943) p. 340

33. Fisher, J.C. Acta Met 1 (1953) p. 32

34. Pascover, J.S. and Radcliffe, SU Acta Met 17 (1969) p. 321

35. Kurdjumov, G.U., JISI, 1960 p. 26

36. Greninger, A.B. Trans AIME 133 (1939) p. 204

37. Mehl, R.F. and Smith, O.W. Trans AIME 113 (1934) p. 203

38. Phillips, A.H., Trans AIME 89 (1930) p. 194

39. Owen, W.S. and Gilbert, A. JISI 196 (1960) p. 142

40. Massalski, T.B. Acta Met 6 (1958) p. 243

41. Saburi, T. and Wayman, C.M. Trans AIME 233 (1965) p. 243

42. Kittl, J.E. and Massalski, T.B. Acta Met 15 (1967) p. 161

43. Gomersall, D.W. and Parr, J.G., JISI 203 (1965) p. 275

44. Wallbridge, J.M. and Parr, J.G. JISI 204 (1966) p. 209

45. Saymen, C.M. et al, J. Applied Physics 341 (1963) p. 2842

46. Parr, J.G. "The Criterion Of The Martensite Transformation" in The History of Metallurgy, AIME (1965) p.125

47. Greninger, A.B. ASM Trans Q, 30 (1942) p. 1

48. Singh, K.P. and Parr, J.G. Acta Met 9 (1961) p.1073

49. Owen, W.S., Wilson, E.A. and Bell, T. "The Structure and Properties of Quenched Iron Alloys" in High Strength Materials (ed. Zackay, U.F.) (John Wiley & Sons Inc., New York, 1965)

50. Paps, H. and Massalski T.B., Acta Met. 13 (1965) p. 1023

51. Owen, W.S. and Bell, E.A., Special Report 93, Iron and Steel Inst. (1965) p. 1-29

52. Yeo, R.G., Trans AIME 224 (1962) p. 1222

53. Barrett, C. and Massalski, T.B. Structure of Metals (3rd ed) (McGraw Hill Publishing Company, New York 1966)

54. Roberts, S.C. Trans AIME (1953) p. 203

55. Kaufman L, and Cohen, M. Prog. Met. Phys. 7 (1958) p. 165

56. Pascover, J.S. and Radcliffe, S.U. Trans AIME 242 (1968) p. 673

57. Greninger, A.S. and Troiano, A.R. ASM Trans Q. 28 (1940) p. 537

58. Bibby, M. Master's Thesis, University of Alberta, (1963)

59. Smith, R.P. Phil Mag 68 (1946) p. 1163

60. Huber, F.E. Chemist-Anclipt, 55, 2 (1966) p. 47

61. Greninger, A.R. Trans ASM 30 (1942) p. 1

62. Duwez, P. Trans AIME 3 (1951) p. 754

63. Srivastava, L.P. and Parr, J.G. Trans AIME 224 (1962) p. 1245

64. Darken, L.S. and Smith, R.P. Inc. L'-ng Chem 43 (1951) p. 1815

65. Smith, R.P., J. Am Chem Soc 68 (1946) p. 1163

66. Digges, T.G. ASM Trans Q (1940) p. 575

67. Anderson, P.D. and Hultgren, R. Trans AIME 224 (1962) p. 842

68. Cody, G.D. Abeles, B. and Beers, D.S. Trans AIME 221 (1961) p. 25

69. Goldschmidt, H.J. Interstitial Alloys (Plenum Press, New York, 1967) p. 66

70. Bonse, U. "X-Ray Picture of the Field of Lattice Distortion Around Single Dislocations" in Direct Observations of Imperfections in Crystals (ed. Newkirk and Wernick) (Interscience Publishers, New York 1962) p. 431

71. Smith, E. In Direct Observation of Imperfections in Crystals (Interscience Publishers, New York, 1962) p. 203

72. Maringer, R.E., Sovik, J.H. and Rengstorff, G.W.P. Unpublished Work (Battelle Memorial Institute, Columbus Ohio)

73. Falquero, E.A. PhD. Thesis, University of Windsor, 1969

74. Esser, H. Eilender, W. Riedel, K., Spenle, E., Ueberdie Stahlhartung, Archiv Eisen 6 (1933) p. 389

APPENDIX I

Alloy Preparation

For this investigation, it was necessary to prepare iron-carbon alloys with carbon contents in the range 5 to 200 ppm by weight. Initially, a method was developed which was based on the reaction of stoichiometric amounts of methane gas with iron in a partially evacuated chamber. After the amount of gas was measured by pressure determinations, the reaction vessel was isolated from the rest of the system and heated to the carburizing temperature for a time sufficient for complete reaction. However, this method produced unpredictable and unreproduceable results, and was abandoned.

A method based on essentially the same principle has proved successful (58) but the cost of building the necessary system could not be justified on the basis of sample preparation for a single project of this nature.

Further attempts were made to use kinetic data available in the literature, but it was found that the derivations and experimental techniques by which these were collected were totally unsuccessful in producing predictable results for the carburization of iron.

The method by which successful alloys were produced for this investigation depends upon the controlled decarburization of a homogeneous iron sample of

approximately eutectoid composition. The method is straightforward and utilizes and apparatus of simple design.

Material:

The starting material was "High Purity Iron" supplied by Battelle Memorial Institute in one pound ingots, 2½ inches in diameter and 6 inches long. A complete chemical analysis is given in Appendix II.

Fabrication of Sheet Samples:

Discs of the high purity iron 0.1 inches thick were cut from the ingot with a high-speed liquid cooled cuff-off saw (Buehler, Model 1010), and cold-rolled to sheet 0.01 inches thick. In order to mininize contamination, the rolls were thoroughly cleaned with acetone. No intermediate annealing was necessary during the rolling operation.

The following procedure was followed in the carburization process (specimen size was 6" x 2" x 0.10):

1) The specimen was attached to a piece of nichrome wire and placed in the cold end of a sealed quartz furnace tube.
2) The furnace tube was flushed with argon.
3) The methane flow was adjusted to a rate of 1 cc per minute.

4) The furnace was heated to 870°C and the system was allowed one hour to come to equilibrium.

5) The specimen was pushed into the hot zone of the furnace tube for 5 minutes.

6) The specimen was pulled back to the cold end of the furnace and the methane flow was replaced by an argon flow of approximately 200 cc per minute while the sample cooled for 10 minutes.

Optical metallography revealed a carbon penetration of 0.002 inches into the specimen surfaces and the carburized layer appeared to be of approximately eutectoid composition (0.8% carbon).

Homogenization:

It was found necessary to homogenize the samples prior to decarburization since the kinetics of the decarburization process are such that complete decarburization takes place in a few seconds unless the carbon is first diffused throughout the sample.

Homogenization was accomplished by sealing the carburized sample in a quartz tube under argon at low pressure and annealing for 30 hours at 1050°C in a furnace specially constructed to minimize non-homogeneous carbon distribution due to thermal diffusion. This furnace had a temperature gradient of less than 2°C over the 8 inches of its centre zone.

Decarburization:

The homogenized specimens were decarburized in "wet" hydrogen in a similar manner to the carburization

process. The following procedure was followed:

1) The specimen was placed in the quartz furnace tube and the hydrogen flow rate adjusted to 8 cc/min.

2) With the furnace tube remaining outside the furnace, the furnace was preheated to 925°C.

3) The furnace tube was placed in the preheated furnace and held for times varying from 2 minutes to 30 minutes. The times were measured from the point at which the thermocouple adjacent to the furnace tube recorded a temperature of 925°C.

4) After the appropriate time at temperature, the furnace tube assembly was taken from the furnace and allowed to cool in air for one hour. The sample remained in the tube and a constant hydrogen flow was maintained.

The amount of carbon present was again determined metallographically under an effective magnification of 1600X (samples were etched with 1 pct nitol). At this point, carbides present were in the form of spheroids and it was found that no carbides were visible at less than 25 ppm carbon. After some experience, it was possible to estimate carbon contents in the region of 30 to 100 ppm to within $\pm$ 5 ppm (based on the analyses carried out at Battelle Memorial Institute)

Rehomogenization:

After the decarburization treatment, the samples were resealed in quartz and given a second anneal at 1050°C for 30 hours.

APPENDIX II

The bar analysis of the high purity iron used in the present investigation is as follows (concentrations are expressed in ppm by weight):

Nonmetallic impurities:

Oxygen	1.4
Nitrogen	
vacuum fusion	0.06
internal friction	0.2
Carbon	
combustion-conductometric	5
internal friction	2.1
Sulfur	
mass spectrometer	none (<0.12)
Total nonmetallics	6.8

Metallic impurities detected:

Arsenic	1.0
Calcium	0.02
Chromium	3.0
Cobalt	5.0
Columbium	0.5
Copper	3.0
Germaniun	2.5
Manganese	0.3
Molybdenum	0.7
Nickel	4.0

Platinum	0.4
Phosphorus	5.0
Potasium	0.02
Sodium	0.02
Titanium	2.5
Tungsten	0.25
Vanadium	0.01
Total metallics detected	30

APPENDIX III

Carbon Analysis

All specimens used in this investigation were analyzed for carbon by Battelle Memorial Institute in Columbus Ohio by the "Combustion-Conductometric method" (60). In essense, this method involves burning the metal specimen and collecting the combustion gases. The carbon dioxide present in these gases is absorbed by a barium hydroxide solution and the conductivity of the solution is measured to give a quantitative measurement of the total carbon content of the original metal specimen. A typical accuracy for this method for a dilute binary iron-carbon alloy is $\pm$ 1 ppm in a sample containing 10 ppm carbon.

Specimens used in this investigation were cut length-wise such that a strip $\frac{1}{4}$" x 6" x 0.01" was available for analysis, the remainder being used for the determination of the transformation temperatures. Initially, duplicate analysis were conducted on material cut from both sides of the sample. However, it became evident the samples were homogeneous, and this practice was discontinued.

Alloy System	Structure Change
Fe-C	fcc-bct
Fe-Ni	fcc-bct
Fe-Ni-C	fcc-bct
Fe-Mn	fcc-bcc (α')
Cu-Zn	bcc-unknown
Cu-Zn-Pb-Sn	bcc-fcc
Cu-Sn	bcc-unknown
Cu-Al	bcc-hcp (distorted)
Li (pure)	bcc-hcp
Zr (pure)	bcc-hcp
Ti (pure)	bcc-hcp
Au-Cd	bcc-orthorhombic
Co (pure)	fcc-hcp
In-Tl	fcc-fct

TABLE 1: Occurrence of the Martensite Transformation.(28)

Reference	M_s (°C)	Cooling Rate (°C/sec)	Metal Analysis (%)
Esser et al. (74)	520	18,000	Carbon 0.017 no record of metallics
Owen and Gilbert (39)	545	5,500	C 0.010 Si 0.005 O_2 0.006 S^2 0.004 P 0.002
Duwez (62)	750	12,000	Carbon 0.001 Trace metallic impurities each < 0.001
Srivastava and Parr (63)	519	10,000	C 0.005 Si 0.02 Ni 0.06

TABLE 2: M_s Values Obtained Prior To Bibby and Parr's Investigation.(18)

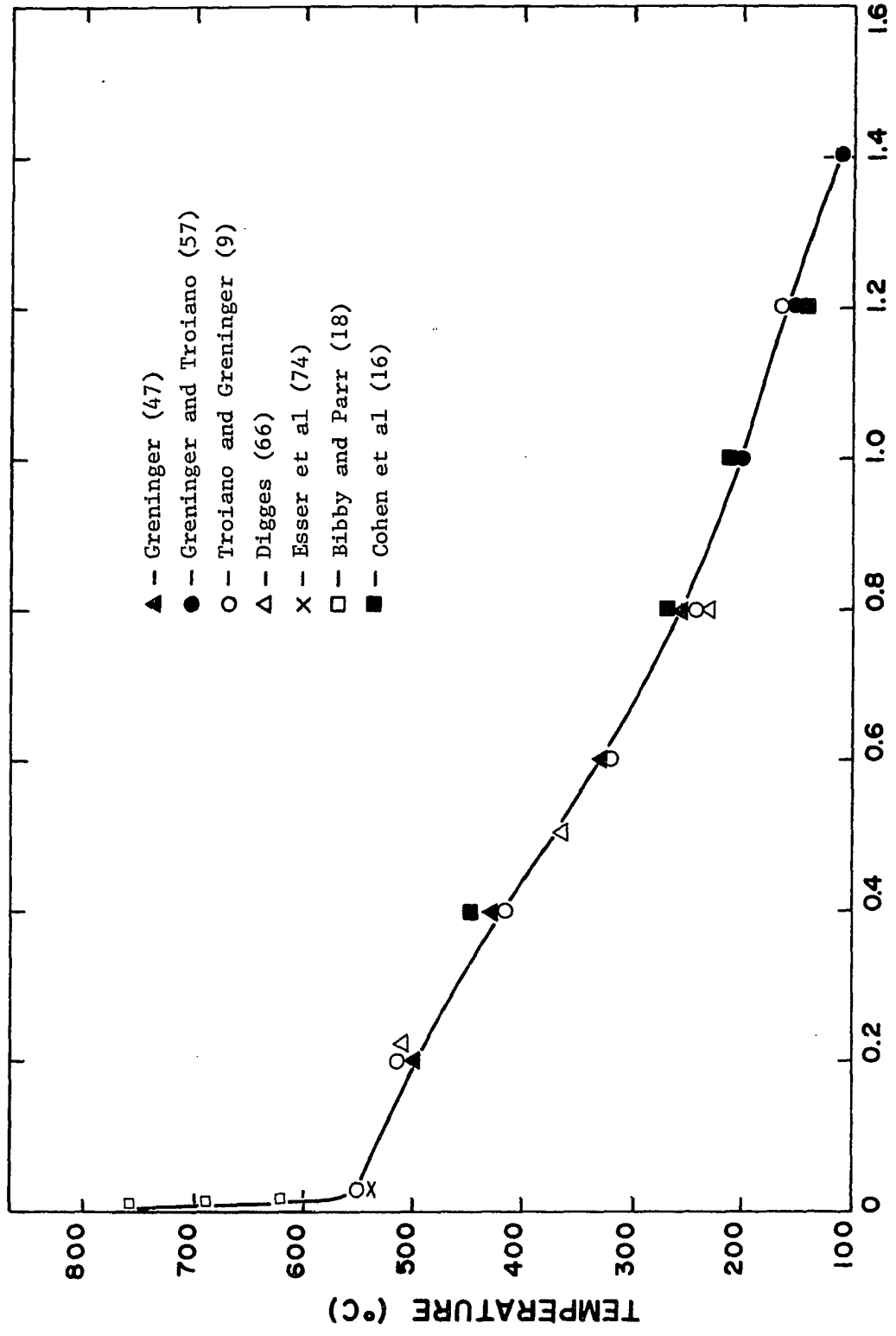

FIG.1 Martensite Transformation Start Temperature (M_s) For The Iron Carbon System Versus Carbon Content

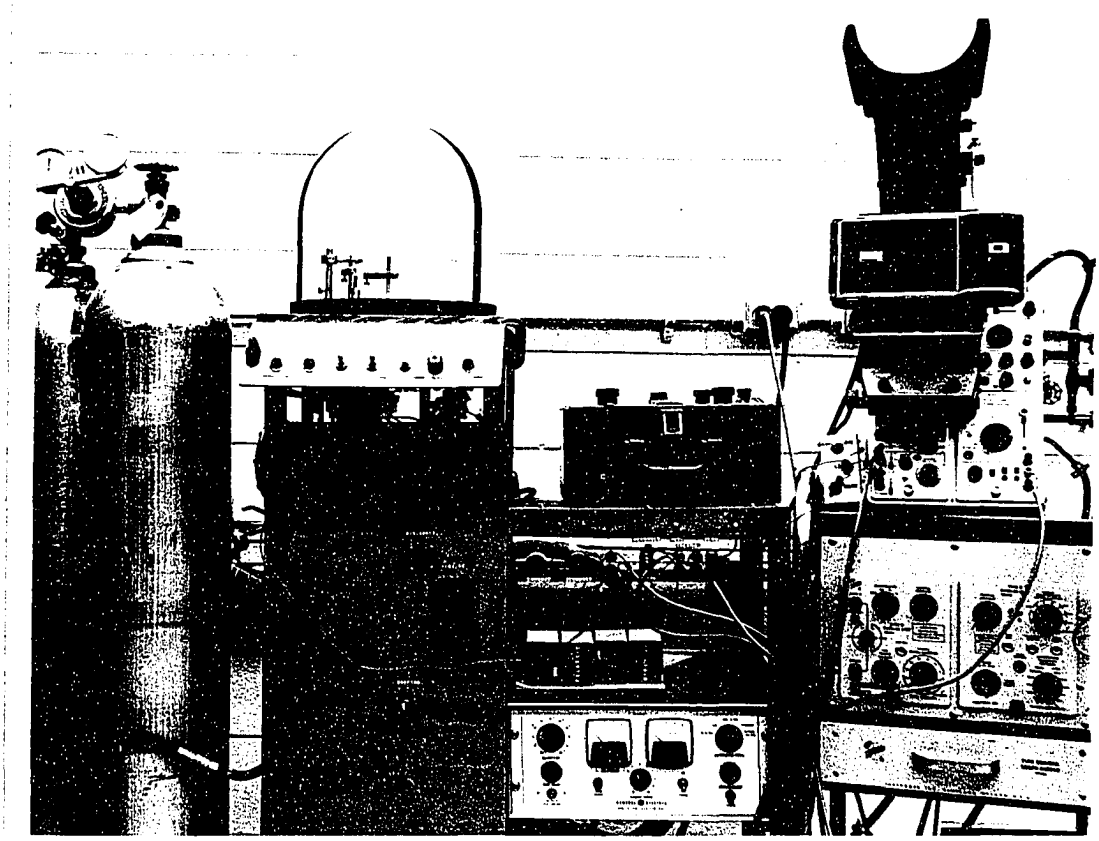

FIG.2 Gas Quenching Assembly

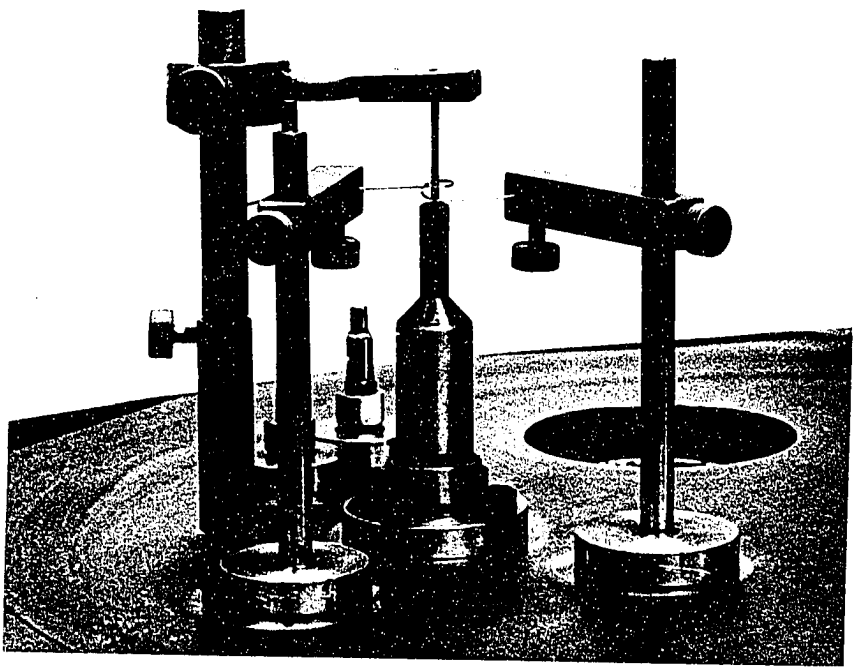

FIG.3 Detail of Gas Quenching Unit

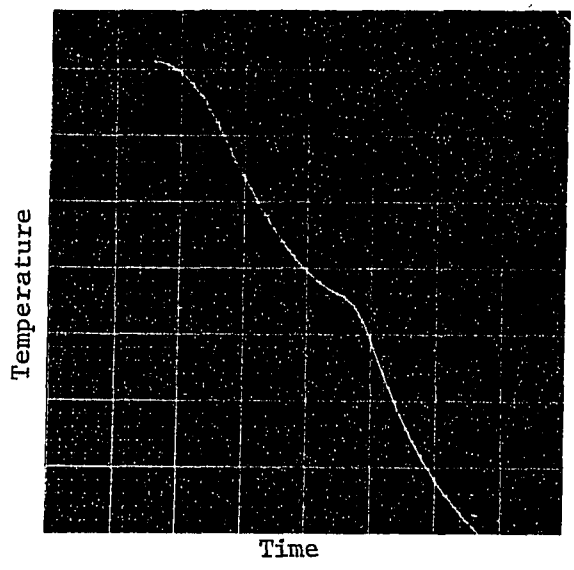

FIGURE 4 Oscilloscope Trace Of Cooling Curve For Iron Sample Containing 143 PPM Carbon (Cooling Rate = 47,500°C/sec Transformation temp = 585°C)

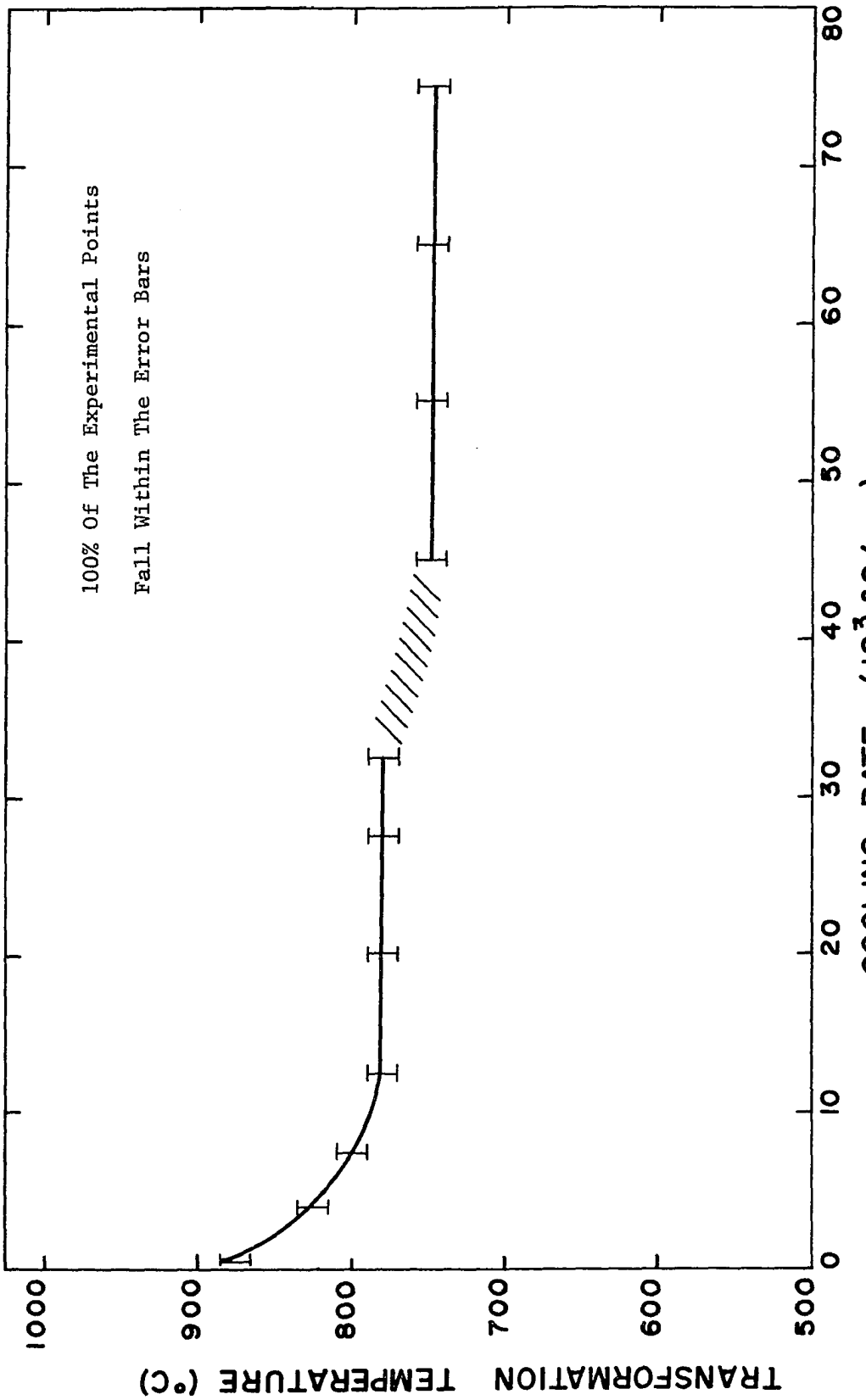

FIG.5 Transformation Temperature Versus Cooling Rate For Fe-15 ppm C

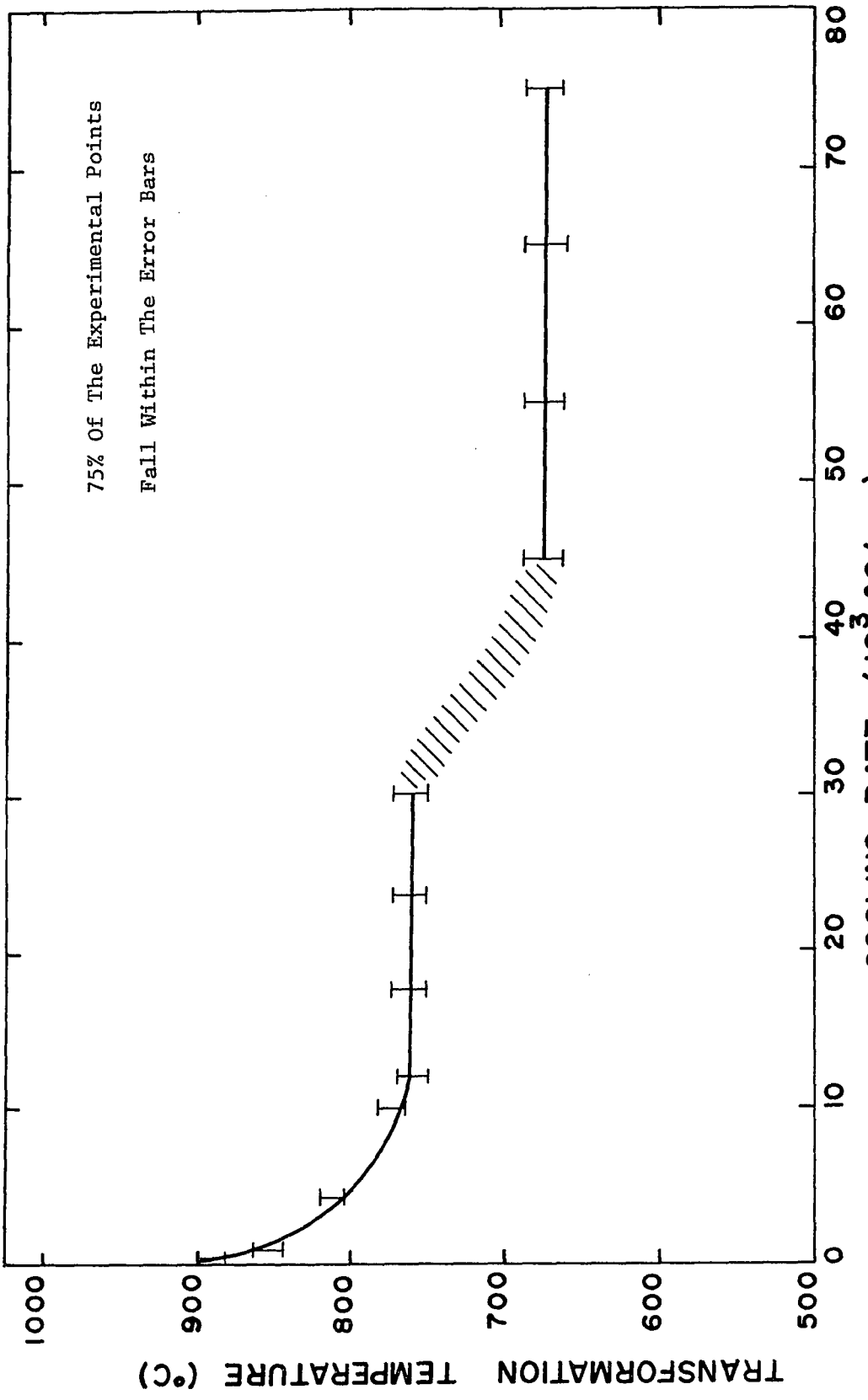

FIG.6 Transformation Temperature Versus Cooloing Rate For Fe-53 ppm C

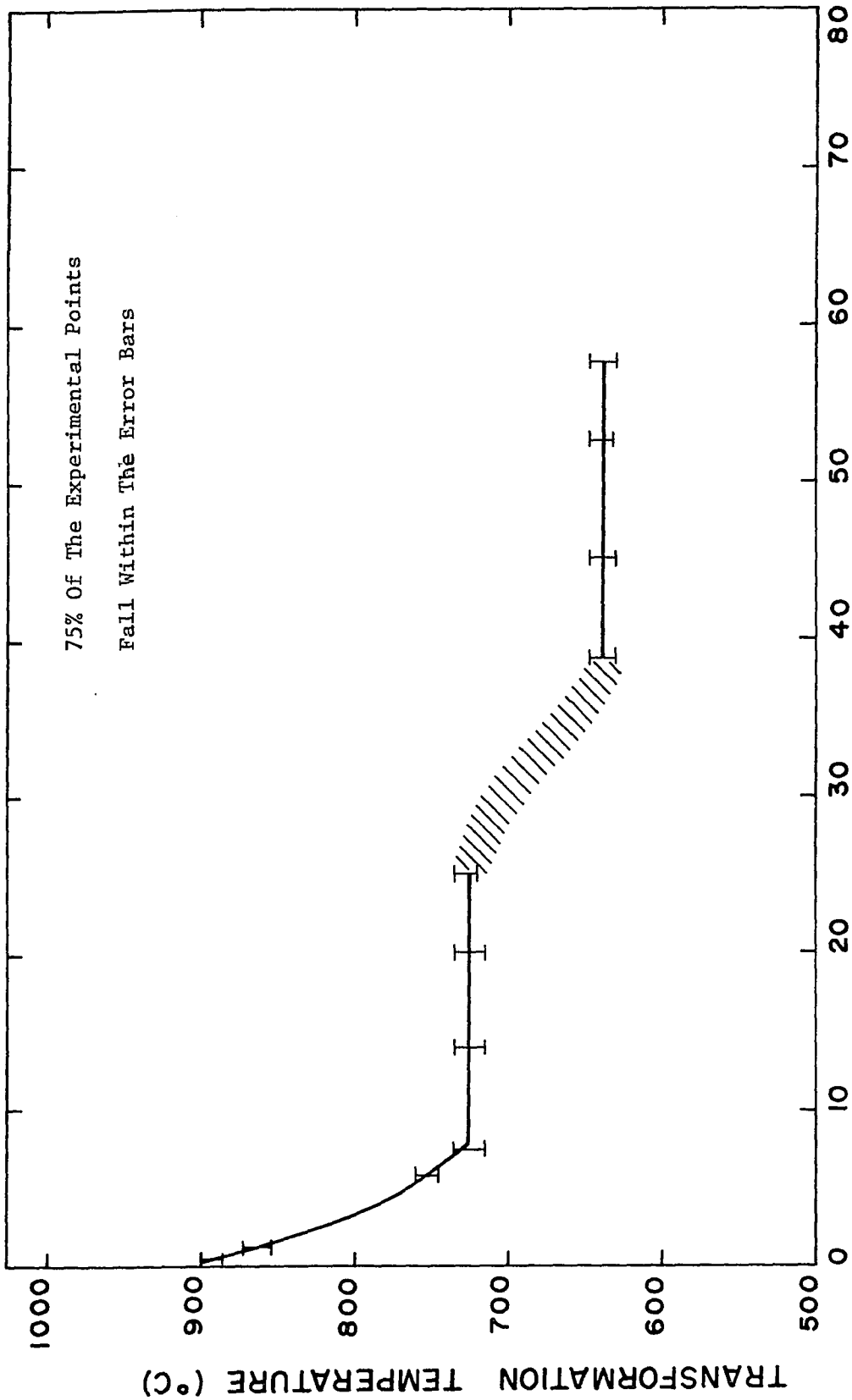

FIG.7 Transformation Temperature Versus Cooling Rate For Fe-105 ppm C

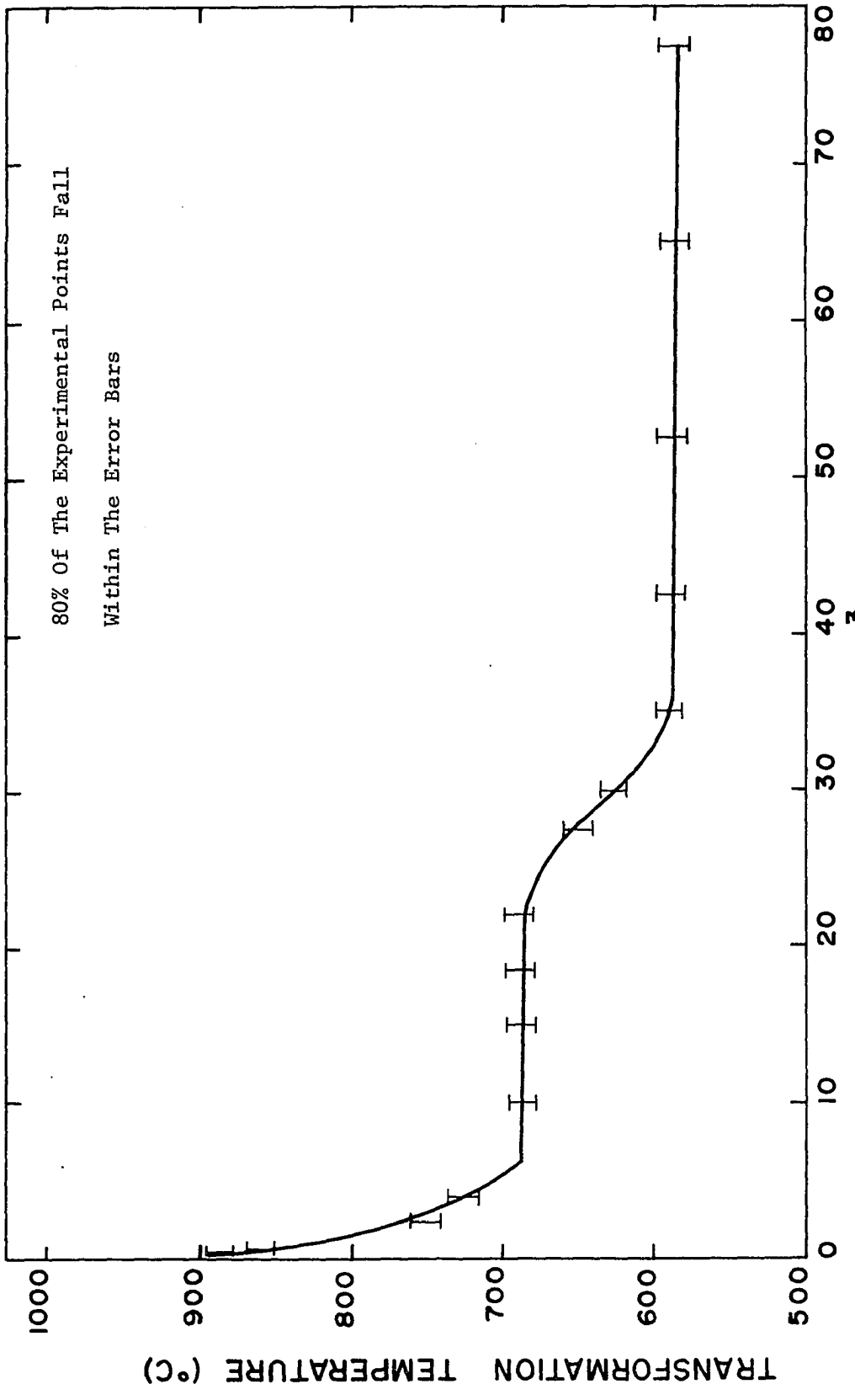

FIG.8 Tranformation Temperature Versus Cooling Rate For Fe-143 ppm C

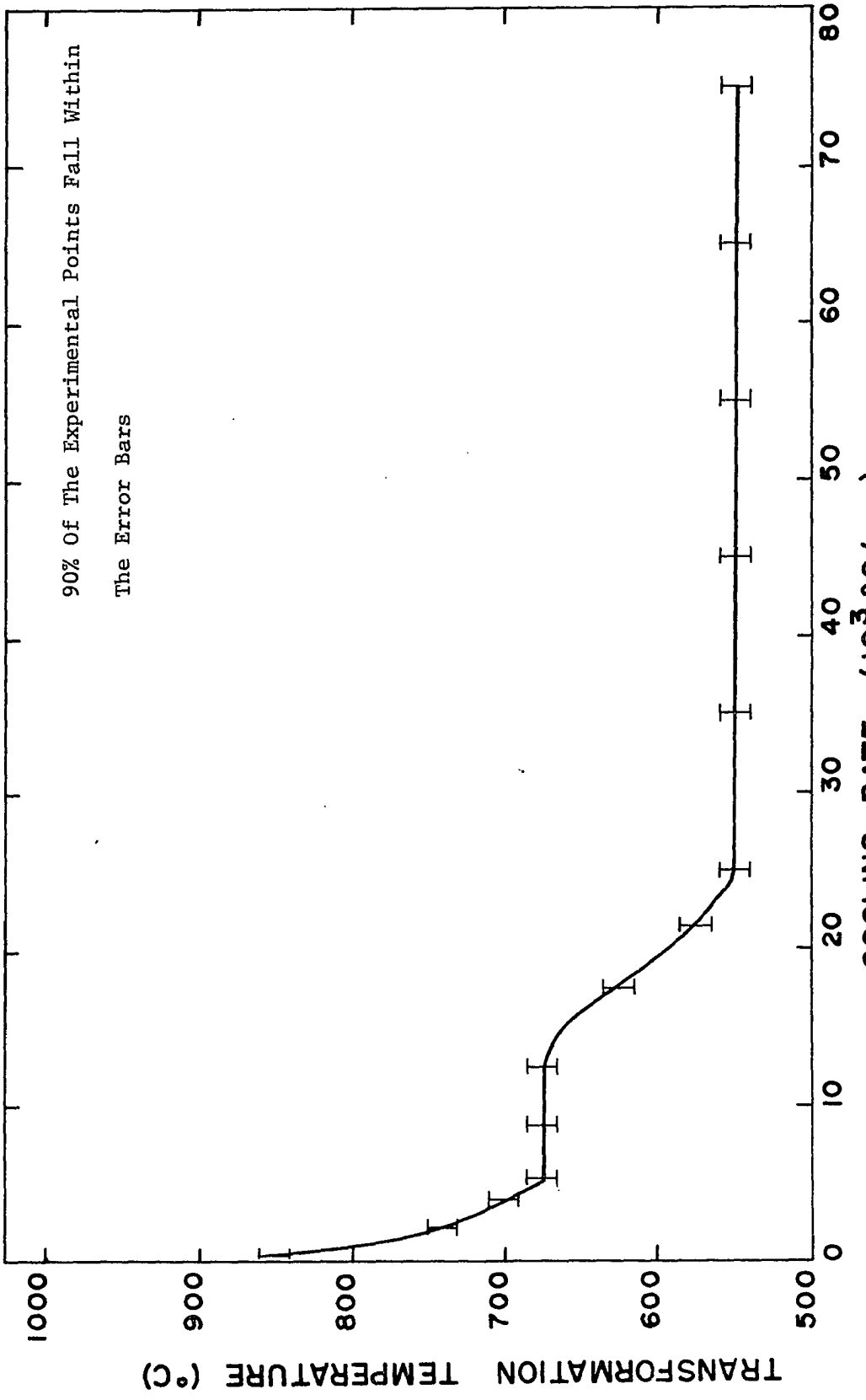

FIG.9 Tranformation Temperature Versus Cooling Rate For Fe-187 ppm C

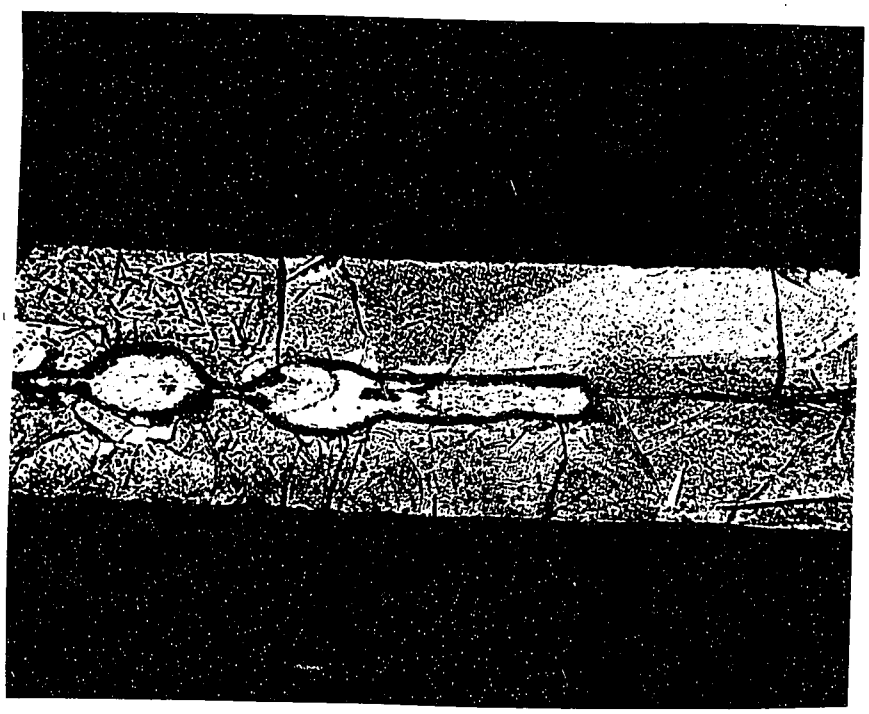

FIG. 10 Iron-20 ppm Carbon Sample Transformed at 125°C/sec. (x160).

FIG. 11 Iron - 20 ppm Carbon Sample Transformed at 20,000°C/sec. (x160).

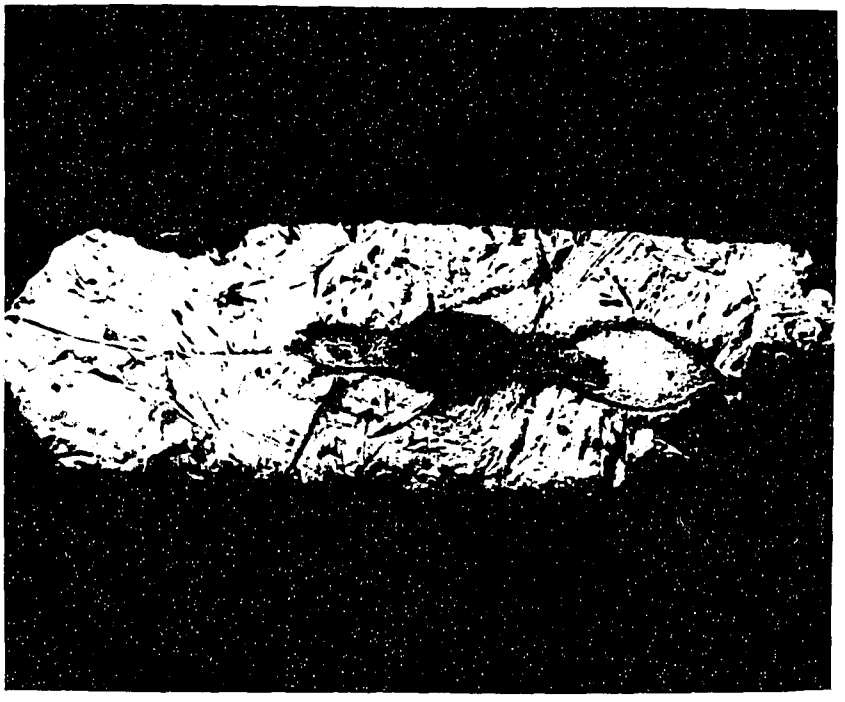

FIG. 12 Iron - 20 ppm Carbon Sample Transformed at 53,000°C/sec. (x160).

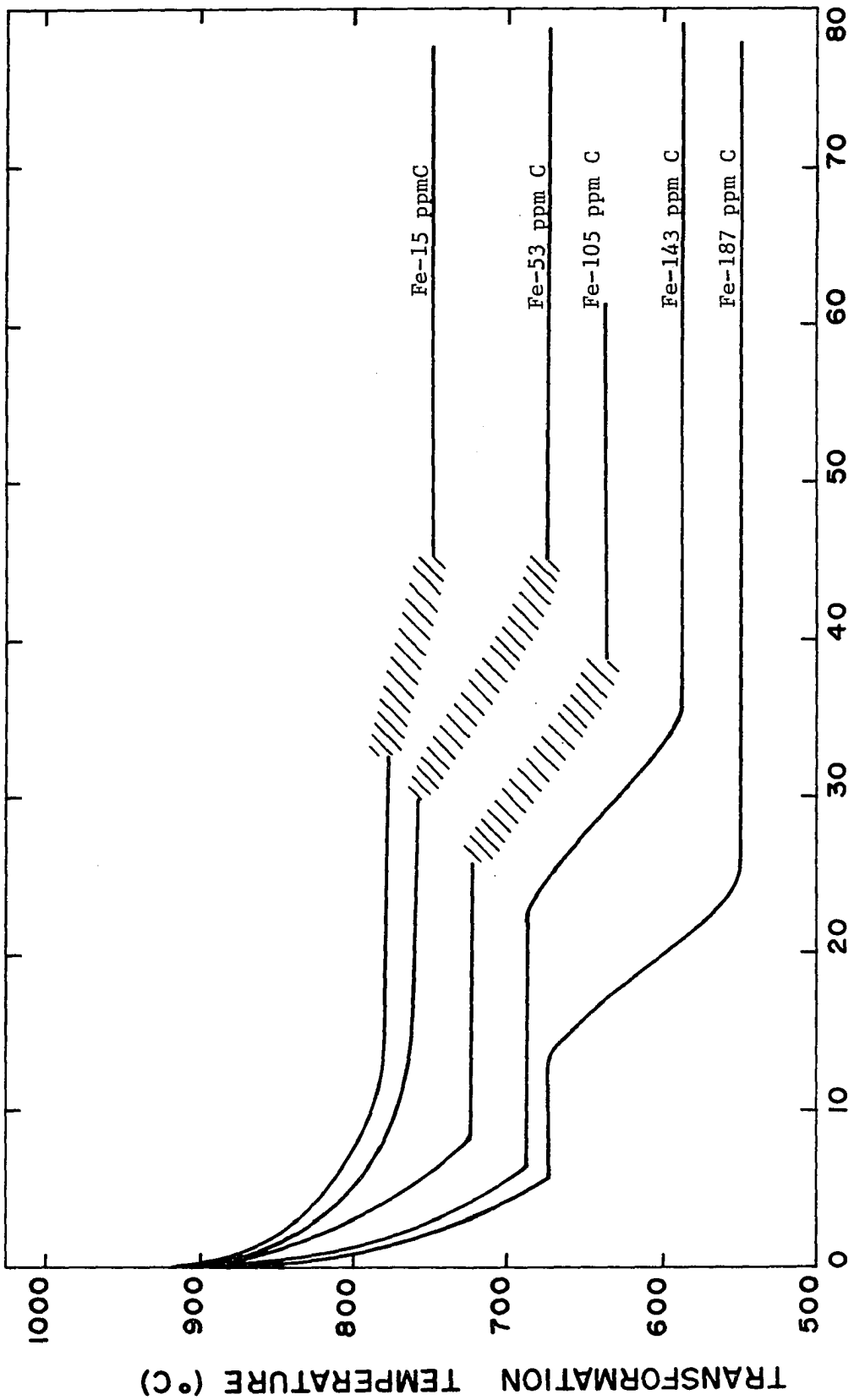

FIG.13 Tranformation Temperature Versus Cooling Rate For Very Dilute Fe-C Alloys

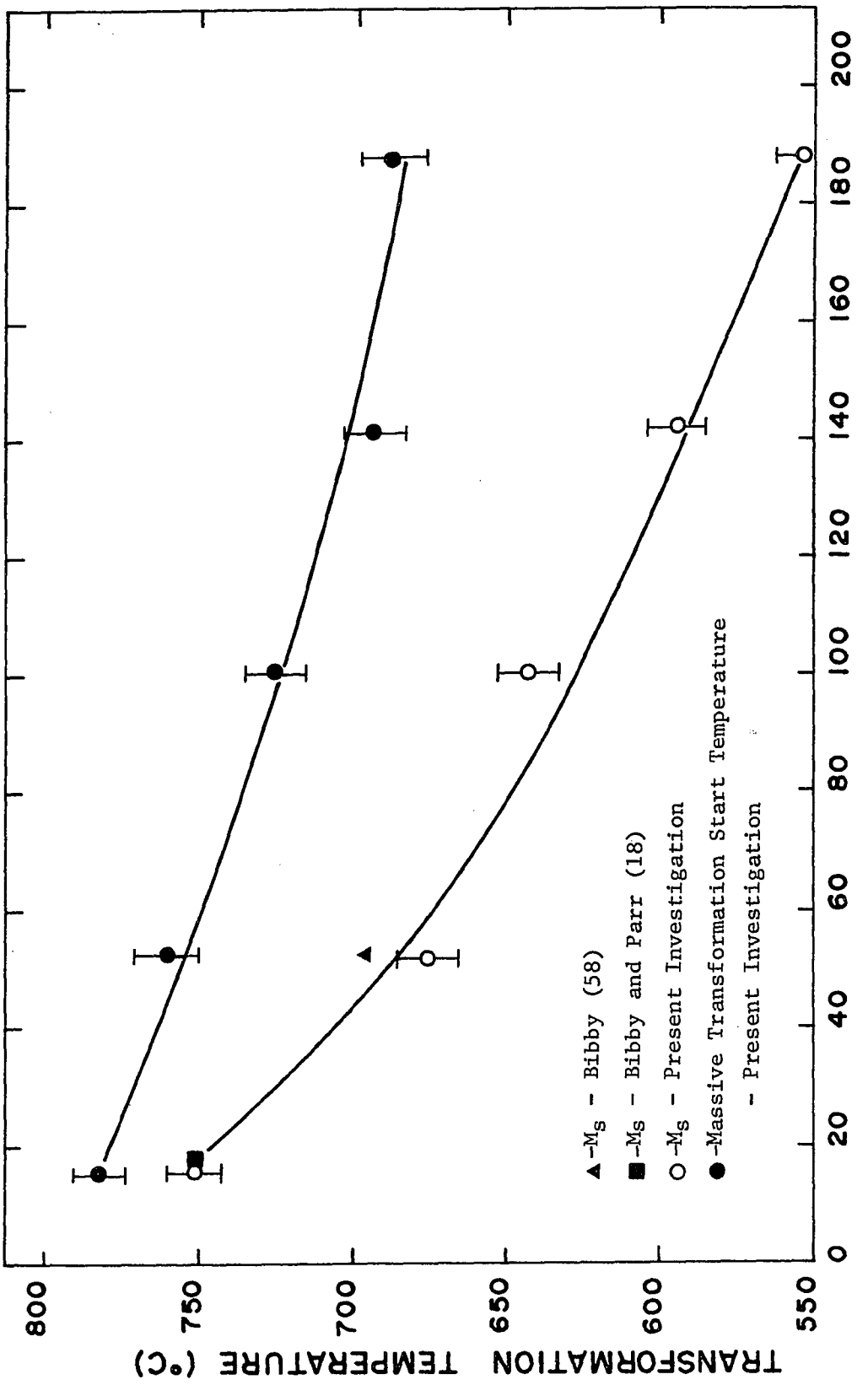

FIG.14 Massive and Martensitic Transformation Temperatures In Very Dilute Fe-C Alloys Versus Carbon Content

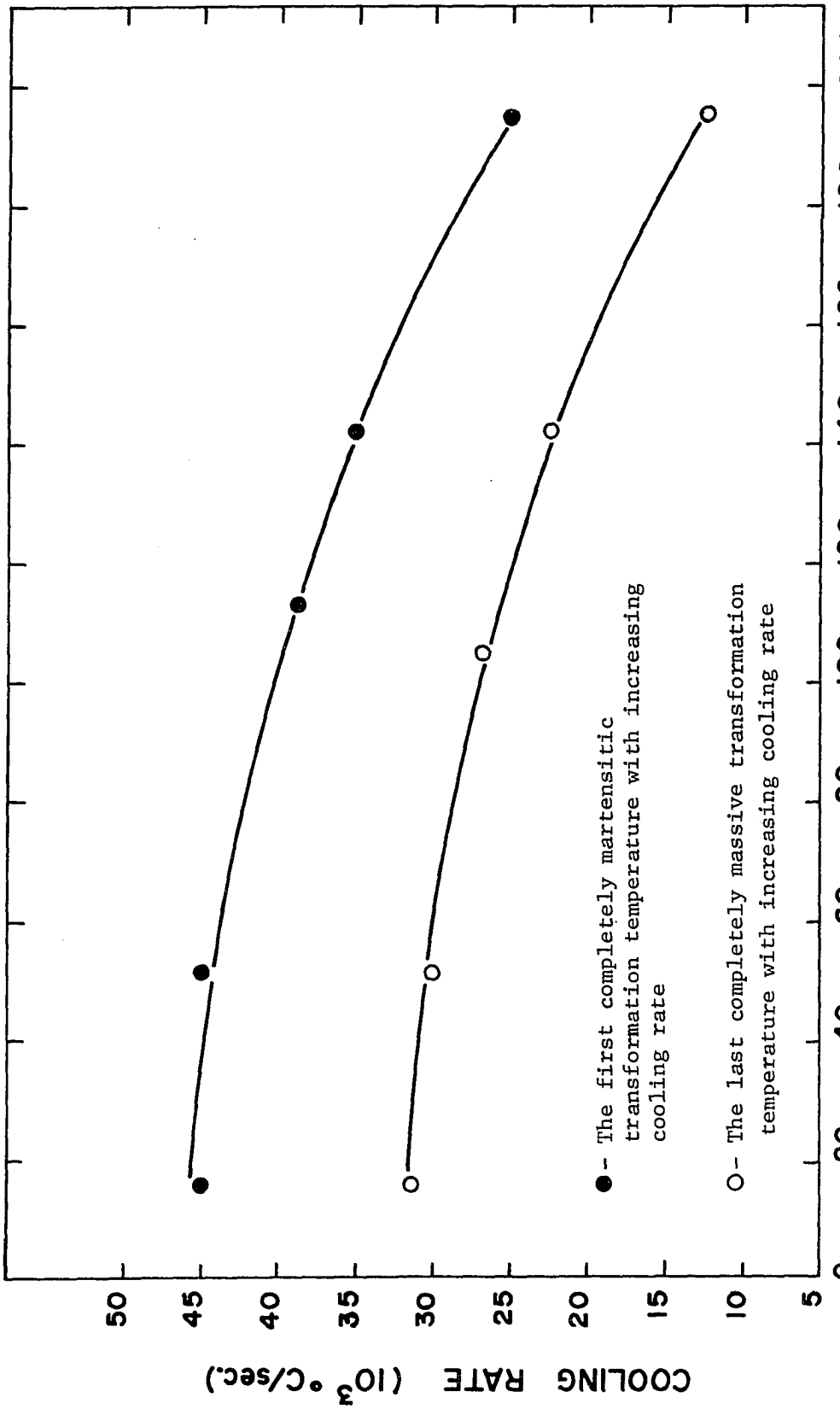

FIG.15 The Dependence Of The Critical Cooling Rate To Obtain Martensite Versus Carbon Content

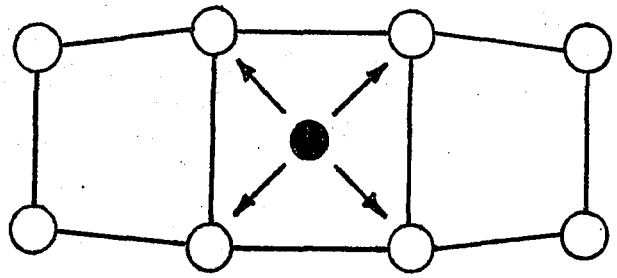

FIG. 16 The Effect Of One Carbon Atom On A Two-Dimensional Iron Array.

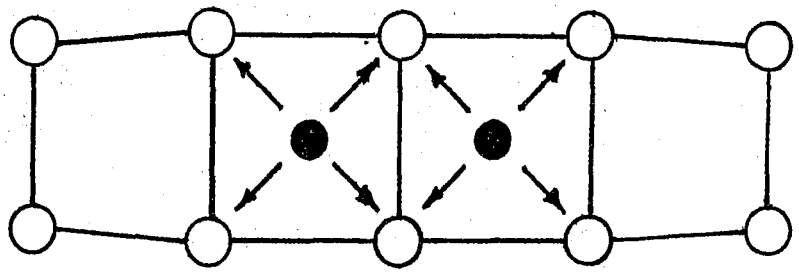

FIG. 17 The Effect Of Two Carbon Atoms In Neighbouring Interstitial Sites Of A Two-Dimensional Iron Array .

VITA AUCTORIS

1944	Born in Toronto, Ontario.
1961	Graduated from Tecumseh High School, Chatham, Ontario.
1964	Graduated from Chatham Collegiate Institute, Chatham, Ontario.
1968	Graduated from University of Windsor with degree of B.Sc. in Engineering Materials.
1968	Accepted into the Graduate School of the University of Windsor as a candidate for the degree of M.A.Sc. in Engineering Materials.